Gold as hydrogen: Structural and electronic properties and chemical bonding in $Si_3Au_3^{+/0/-}$ and comparisons to $Si_3H_3^{+/0/-}$

Boggavarapu Kiran,[a)] Xi Li,[b)] Hua-Jin Zhai, and Lai-Sheng Wang[c)]
*Department of Physics, Washington State University, 2710 University Drive, Richland, Washington 99354
and Chemical Sciences Division, Pacific Northwest National Laboratory, P.O. Box 999, MS K8-88,
Richland, Washington 99352*

A single Au atom has been shown to behave like H in its bonding to Si in several mono- and disilicon gold clusters. In the current work, we investigate the Au/H analogy in trisilicon gold clusters, $Si_3Au_3^{+/0/-}$. Photoelectron spectroscopy and density functional calculations are combined to examine the geometric and electronic structure of $Si_3Au_3^-$. We find that there are three isomers competing for the ground state of $Si_3Au_3^-$ as is the case for $Si_3H_3^-$. Extensive structural searches show that the potential energy surfaces of the trisilicon gold clusters ($Si_3Au_3^-$, Si_3Au_3, and $Si_3Au_3^+$) are similar to those of the corresponding silicon hydrides. The lowest energy isomers for $Si_3Au_3^-$ and Si_3Au_3 are structurally similar to a Si_3Au four-membered ring serving as a common structural motif. For $Si_3Au_3^+$, the 2π aromatic cyclotrisilenylium auride ion, analogous to the aromatic cyclotrisilenylium ion ($Si_3H_3^+$), is the most stable species. Comparison of the structures and chemical bonding between $Si_3Au_3^{+/0/-}$ and the corresponding silicon hydrides further extends the isolobal analogy between Au and H. © 2006 American Institute of Physics. [DOI: 10.1063/1.2216707]

I. INTRODUCTION

Gold possesses unusual and diverse chemistries among the coinage metals due to the relativistic effects.[1–3] Relativistic stabilization of the $6s$ orbital leads to an anomalously high electron affinity for Au, comparable to those of the halogens. Consequently, many auride (Au⁻) compounds exist,[4] in which Au acts as the electron acceptor. New molecules with Au acting as halogens have also been proposed.[5] One of the most interesting properties of gold is the isolobal analogy between a gold phosphine unit (AuPR₃) and a hydrogen atom in compounds such as C(AuPR₃)₄ and C(AuPR₃)₅⁺.[6–13] However, the analogy between a single Au atom and a H atom has not been discovered until very recently from our laboratory.[14–16] We first observed that the structures and chemical bonding of a series of $SiAu_n$ clusters are similar to those of SiH_n ($n=2–4$) and that $SiAu_4$ is a stable tetra-auride molecule with a large highest occupied molecular orbital-lowest unoccupied molecular orbital (HOMO-LUMO) gap analogous to SiH_4.[14] We further showed experimental and theoretical evidence that the structures and isomers of Si_2Au_2 and Si_2Au_4 are analogous to those of Si_2H_2 and Si_2H_4, respectively.[15] Very recently we have shown that the structure and bonding of B_7Au_2 are identical to those of B_7H_2.[16] The Au/H analogy in Si–Au and B–Au alloy clusters is originated from the similar electronegativity between Si/B and Au. The concept of Au/H analogy may be a general phenomenon in Au-alloy clusters

and adds a new dimension to the expanding chemistry of Au. Several recent theoretical works have further explored the Au/H analogy.[17,18]

In the current study, we intend to examine the generality of the Au/H analogy in larger Si–Au clusters. To establish the Au/H analogy in larger Si–Au clusters is of practical importance. With increasing cluster size, the potential energy surfaces of the binary clusters become more complicated and the number of possible geometric combinations becomes enormous. Therefore, it is highly desirable to develop structural guidelines and chemical intuitions that may help identify possible structural patterns for a given stoichiometry.

Our focus here is on the Si_3Au_3 cluster in its various charged states, for which very little is known either experimentally or theoretically. Fortunately, the corresponding $Si_3H_3^{+/0/-}$ species have received considerable research attention in the past decade, primarily due to the importance and potential applications of silicon hydrides in semiconductors, optoelectronics, and related technological areas.[19,20] In particular, earlier *ab initio* studies showed that the most stable structure for $Si_3H_3^+$ is the cyclotrisilenylium ion, which is a 2π aromatic system.[21–25] A compound containing the cyclic Si_3^+ aromatic ring has been synthesized very recently with bulky ligands.[26] A recent *ab initio* study has explored the potential energy surfaces extensively and identified numerous structural isomers for Si_3H_3 and $Si_3H_3^-$.[27] These prior studies on $Si_3H_3^{+/0/-}$ provide a solid background for the current work to further explore the Au/H analogy. We investigated the structures and bonding in $Si_3Au_3^{+/0/-}$ using both anion photoelectron spectroscopy (PES) and density functional theory (DFT). We show that the Au/H analogy clearly holds in the trisilicon clusters; and the structures and chemi-

a)Present address: Physics Department, Virginia Commonwealth University, Richmond, VA 23284.
b)Present address: Rowland Institute at Harvard, 100 Edwin H. Land Blvd., Cambridge, MA 02142.
c)Electronic mail: ls.wang@pnl.gov

cal bonding of $Si_3Au_3^{+/0/-}$ are indeed analogous to those of $Si_3H_3^{+/0/-}$.

II. EXPERIMENTAL AND COMPUTATIONAL METHODS

A. Photoelectron spectroscopy

The experiment was performed using a magnetic-bottle time-of-flight PES apparatus equipped with a laser vaporization supersonic cluster source, details of which have been described previously.[28,29] Briefly, the second harmonic output of a Q-switched Nd:YAG (yttrium aluminum garnet) laser, typically at 10 mJ/pulse and 10 Hz repetition rate, was focused down to a 1 mm spot onto a Au/Si mixed disk target. A helium carrier gas pulse (10 atm backing pressure) was delivered to cool the laser-induced plasma and facilitate cluster formation in the nozzle. The nascent clusters were entrained in the helium carrier gas and underwent a supersonic expansion, which was collimated with a skimmer downstream. Negatively charged clusters were extracted from the cluster beam perpendicularly and analyzed by a time-of-flight mass spectrometer. The cluster anion of interest, $Si_3Au_3^-$, was mass selected and decelerated before being photodetached. Two detachment photon energies were used in the current experiment: 355 nm (3.496 eV) and 266 nm (4.661 eV). Photoelectrons were collected by the magnetic bottle at nearly 100% efficiency and analyzed in a 3.5 m long electron time-of-flight tube. The photoelectron spectra were calibrated using the known spectra of Au^- and Rh^-. The resolution of the apparatus is $\Delta E_k/E_k \sim 2.5\%$, that is, ~ 25 meV for 1 eV electrons.

B. Computational methods

Density functional theory is used in the current theoretical calculations. We employed the Stuttgart quasirelativistic pseudopotentials and basis sets[30–33] augmented with two f-type polarization functions (0.498 and 1.461) for gold[34] and cc-pVTZ basis set for silicon.[35] All the calculations are spin restricted for closed-shell molecules and spin unrestricted for open-shell species. We tested a variety of hybrid and pure density functionals. From our prior experiences on small silicon gold binary clusters,[14,15] we found that the B3LYP functional[36–38] gives reasonable results. For the $SiAu_n^-$ ($n=2–4$) series,[14] we did both CCST(D) and B3LYP calculations previously and found that the B3LYP method gave comparable results as CCST(D). Therefore, all the DFT data reported here correspond to the B3LYP calculations. Frequency calculations were done to confirm that all the obtained structures are true minima. Vertical detachment energies (VDEs) were calculated using time-dependent-DFT (TD-DFT) method based on the anion geometries.[39] All calculations were carried out with GAUSSIAN 03.[40]

III. EXPERIMENTAL RESULTS

Figure 1 shows the photoelectron spectra of $Si_3Au_3^-$ at 355 and 266 nm. The 355 nm spectrum [Fig. 1(a)] shows two intense bands: X (VDE: 2.80 eV) and A (VDE: 3.14 eV). The widths of both bands are significantly broader than the instrumental resolution and they remain the same in
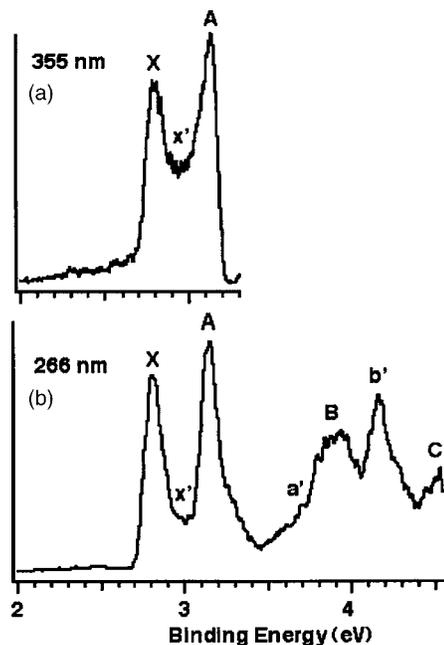

FIG. 1. Photoelectron spectra of $Si_3Au_3^-$ at (a) 355 nm (3.496 eV) and (b) 266 nm (4.661 eV).

the 266 nm spectrum [Fig. 1(b)]. This observation indicates that the observed spectral widths are not limited by the instrumental resolution, but rather due to a geometry change upon photodetachment from the $Si_3Au_3^-$ anion to its corresponding neutral states. Because of the lack of vibrational resolution, the adiabatic detachment energy (ADE) of the ground state transition (X), which also represents the electron affinity of the Si_3Au_3 neutral species, was estimated by drawing a straight line at the leading edge of the X band and then adding the instrumental resolution to the intersection with the binding energy axis. Although this is an approximate procedure, we were able to obtain a consistent ADE from spectra taken at different photon energies. The ADE thus evaluated is 2.71 ± 0.03 eV.

The 266 nm spectrum reveals congested spectral features beyond 3.5 eV. Several broad bands can be tentatively identified and labeled in Fig. 1(b) as a', B, b', and C. Weak spectral features may also be present around 3 eV (x') in between the intense X and A bands, as well as on the higher binding energy side of the A band as a shoulder around 3.3 eV. The congested nature of the PES spectra suggested the presence of multiple isomers, which were confirmed by relative intensity changes upon variation of our experimental conditions and were also born out from our DFT calculations (*vide infra*). The observed ADE and VDEs for $Si_3Au_3^-$ are summarized in Table I, where they are compared with the computational data.

IV. COMPUTATIONAL RESULTS

A. $Si_3Au_3^-$

Numerous isomers were considered to search for the ground state structure of $Si_3Au_3^-$. In addition to the reported minima for $Si_3H_3^-$,[37] several "clusterlike" geometries were

TABLE I. Experimental vertical detachment energies (VDEs) of $Si_3Au_3^-$ and comparison with calculated VDEs for the three low-lying isomers of $Si_3Au_3^-$ (1–3) at B3LYP level. All energy values are given in eV. The calculated ADEs for isomers 1, 2, and 3 are 2.74, 2.80, and 2.64 eV, respectively.

Feature	VDE (expt.)[a]	$1(C_2, {}^1A)$		$2(C_1, {}^1A)$		$3(C_s, {}^1A')$	
		MO	VDE(Theor.)	MO	VDE(Theor.)	MO	VDE(Theor.)
X[b]	2.80(3)					$9a''$	2.76
x'	~2.95	$13a$	3.01	$23a$	3.07		
A	3.14(2)	$10b$	3.16	$22a$	3.26	$14a'$	3.20
a'	~3.65	$12a$	3.71	$21a$	3.64		
B	3.89(5)					$13a'$	3.92
b'	4.15(2)	$11a$	4.16	$20a$	4.09		
C	4.53(2)					$8a''$	4.57

[a]Numbers in parentheses represent the experimental uncertainties in the last digit.
[b]The ground state ADE is measured to be 2.71 ± 0.03 eV, which also represents the electron affinity of the corresponding Si_3Au_3 neutral species.

also included in the structural search. The six most stable isomers (1–6) are presented in Fig. 2, along with their relative energies. The lowest energy structure is the *trans*-dibridged isomer (1) with C_2 symmetry, in which one of the Au atoms forms a rhombus Si_3Au ring with the three Si atoms. The two out-of-plane Au atoms are each unsymmetrically bridging two Si atoms with the shorter and longer Au–Si distances being 2.44 and 2.80 Å, respectively. As will be shown below, the Si_3Au ring appears to be a common structural motif in all $Si_3Au_3^{+/0/-}$ species. Closely followed in energy is a low-symmetry *cis*-isomer (2), which also contains a Si_3Au ring. But the two out-of-plane Au atoms are on the same side of the ring with one bridging and one nonbridging Au atoms. The bridging Au atom becomes somewhat more symmetric (Au–Si distances of 2.48 vs 2.57 Å). The third low-lying isomer (3) is only 0.29 eV higher in energy than isomer 1. Here the two out-of-plane Au atoms are bonded to the same Si atom, which is tetrahedrally coordinated. The three lowest energy isomers of $Si_3Au_3^-$ all possess a Si_3Au ring unit, and the differences between them are the locations of the two out-of-plane Au atoms, which appear to be rather flexible.

Substantially higher in energy lie three isomers 4–6, which are virtually isoenergetic with each other. These isomers can be constructed from a triangular Si_3 ring with two terminal Au atoms bonded to one Si site and the third Au bonded to different positions of the Si_3 ring.

B. Si_3Au_3

An independent structural search was conducted for Si_3Au_3, and the most stable isomers (7–12) are depicted in Fig. 3. The low-lying neutral isomers are similar to the anion (1–6, Fig. 2). The three lowest energy isomers, 7–9, are comparable to the anions 1–3 with a similar energy ordering. However, isomers 10–12 show a reversed energy ordering from the neutral counterparts. Notably, isomer 10, which corresponds to isomer 6 in the anion, becomes more stable in the neutral. There are no substantial differences in the geometric parameters between the neutral and anion isomers, in particular, in the Si–Au bond distances. The Si–Si distance experiences more visible changes, mainly between isomer 3 and the corresponding neutral isomer 9 and between isomer 5 and the corresponding neutral isomer 11, suggesting that the extra electron in the anions occupies a molecular orbital (MO) primarily involving the Si_3 moiety.

C. $Si_3Au_3^+$

The first six low-lying isomers of $Si_3Au_3^+$ (13–18) are shown in Fig. 4, which are quite different from those of the anion or neutral. The most stable structure of $Si_3Au_3^+$ is the aurocyclotrisilenylium ion (13) with D_{3h} symmetry. The Si–Si bond length in 13 (2.23 Å) is shorter than typical Si–Si bonds (~2.4 Å, Figs. 2 and 3) and closer to the Si=Si double bond lengths in Si_2Au_4 and Si_2Au_4.[15] The next isomer
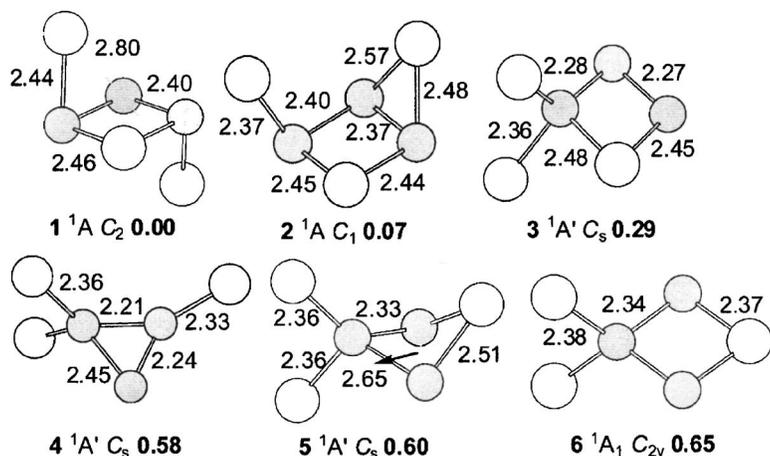

FIG. 2. Optimized structures for $Si_3Au_3^-$ (1–6) at the B3LYP level of theory. Bond lengths are given in Å and the relative energies in eV. The gray balls are Si and the empty balls are Au.
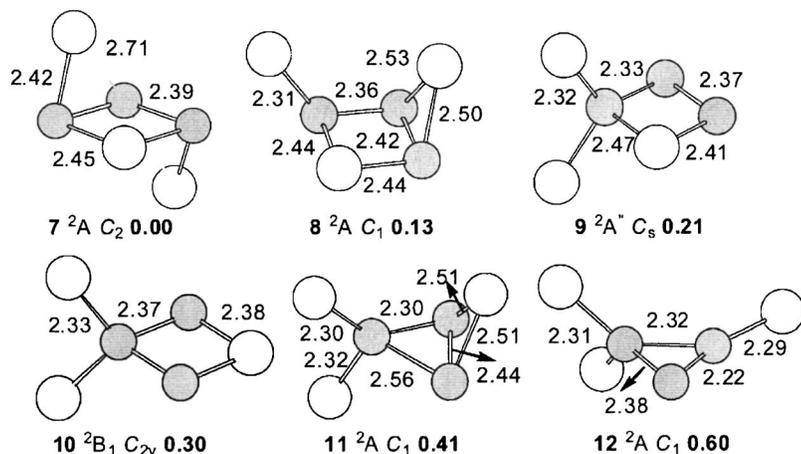
FIG. 3. Optimized structures for Si_3Au_3 (7–12) at the B3LYP level of theory. Bond lengths are given in Å and the relative energies in eV. The gray balls are Si and the empty balls are Au.

(14), in which a Au atom nearly caps a Si_3Au four-membered ring, is virtually isoenergetic to 13 at the current level of theory. Isomer 14 can be derived from neutral isomer 10 by bending one of the terminal Au atoms over the four-membered Si_3Au ring. The third low-lying isomer (15) is completely planar (C_{2v}), which is related to the ground state structure (13) by moving one terminal Au to a bridging position. It also contains a Si_3 ring, whose short Si–Si bond lengths (2.28 Å) are again in between typical Si–Si single bonds and Si=Si double bonds, similar to isomer 13. The remaining isomers (16–18) are slightly higher in the energy ladder and they also have no neutral counterparts.

V. INTERPRETATION OF THE PHOTOELECTRON SPECTRA

On the basis of the current DFT calculations, the three lowest-lying isomers of $Si_3Au_3^-$ (1–3) are energetically very competitive and may all contribute to the observed PES spectra. VDEs for these three isomers were calculated, as given in Table I.

A. Assignments of the main PES features: *X, A, B,* and *C*

The calculated first VDEs of isomers 1, 2, and 3 are 3.01, 3.07, and 2.76 eV, respectively (Table I). Clearly the calculated VDE of 3 is in good agreement with the measured

VDE of the intense *X* band (VDE: 2.80±0.03 eV), whereas that of either 1 or 2 is substantially deviated from the experimental data by 0.2–0.3 eV. Therefore, isomer 3 seems to be the dominant species in our $Si_3Au_3^-$ cluster beam and should be responsible for the main observed PES features.

Isomer 3 is singlet (C_s, $^1A'$) with a valent electronic configuration of $8a''^2 13a'^2 14a'^2 9a''^2$. Its first photodetachment channel is from the $9a''$ HOMO, which primarily consists of a localized Si–Si π bond [Fig. 5(c)]. Electron detachment from the $9a''$ MO reaches the neutral isomer 9. The substantial Si–Si bond length increase from 2.27 Å in anion 3 to 2.37 Å in neutral 9 is consistent with the nature of the $9a''$ MO. The calculated ADE (2.64 eV) from isomer 3 is also in close agreement with the experimental value (2.71 ±0.03 eV).

The second detachment channel of isomer 3 is from the $14a'$ HOMO-1, which is primarily Si–Si σ bonding with some contributions from Si lone pairs [Fig. 5(c)]. The calculated VDE for this transition is 3.20 eV, in excellent agreement with the experimental value of 3.14 eV for the second main PES band *A* (Table I). The next higher binding energy detachment channels are from $13a'$ HOMO-2 and $8a''$ HOMO-3, whose calculated VDEs are 3.92 and 4.57 eV, respectively, and are in good agreement with the VDEs of the broad bands *B* (VDE: 3.89 eV) and *C* (VDE: 4.53 eV). The overall agreement between the calculated detachment channels from isomer 3 and the main PES features (*X, A, B,* and
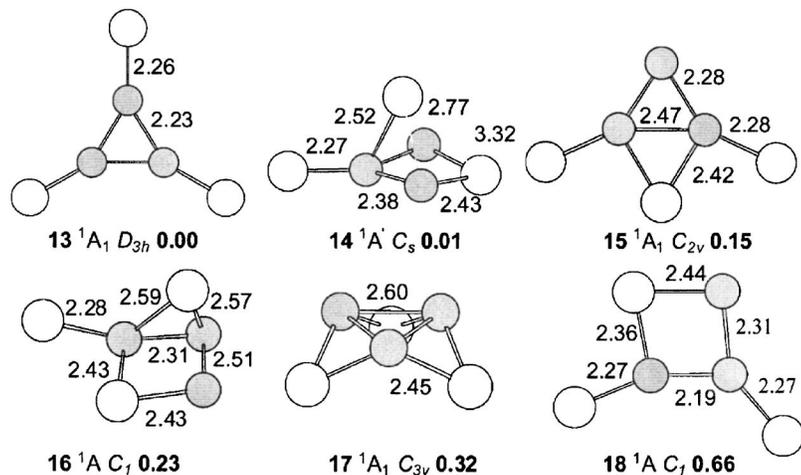

FIG. 4. Optimized structures for $Si_3Au_3^+$ (13–18) at the B3LYP level of theory. Bond lengths are given in Å and the relative energies in eV. The gray balls are Si and the empty balls are Au.
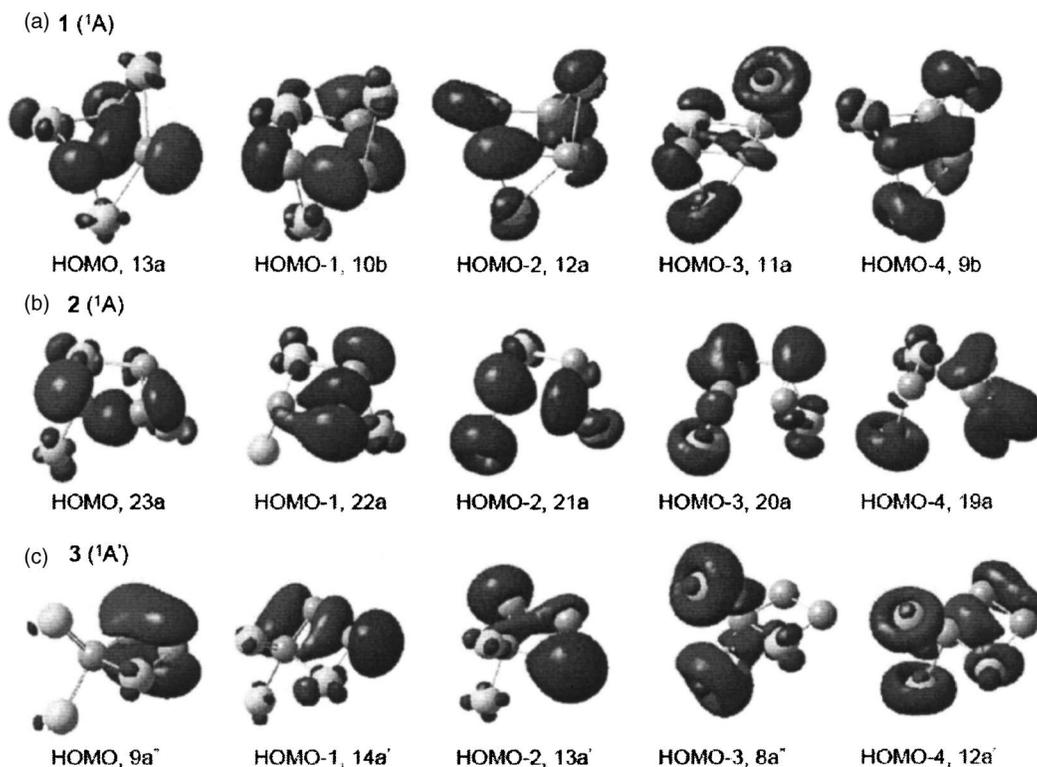
FIG. 5. Valence molecular orbital pictures of the three lowest energy isomers of $Si_3Au_3^-$. (a) isomer 1, (b) isomer 2, and (c) isomer 3.

C) lends considerable credence for the spectral assignment and suggests that isomer 3 is the predominant species in the $Si_3Au_3^-$ beam. Considering the accuracy of the DFT method, we suspect that isomer 3 is very likely to be the global minimum for $Si_3Au_3^-$.

B. Evidence of low-lying isomers

In addition to the main PES features from isomer 3, there are weaker PES features in Fig. 1 (x' and a'), as well as a rather intense feature b'. These features could be either due to contaminations or other isomers of $Si_3Au_3^-$. Due to the near mass degeneracy between one Au atom and seven Si, other Si–Au clusters with stoichiometries, $Si_{10}Au_2^-$ and $Si_{17}Au^-$, as well as Si_{24}^-, all have nearly identical mass as $Si_3Au_3^-$ and could contribute to the PES spectra. Under our experimental conditions, which favor $Si_3Au_3^-$, the silicon-rich clusters $Si_{17}Au^-$ and Si_{24}^- are less likely to be present, but $Si_{10}Au_2^-$ may be present as a minor contributor. Similar mass contaminations have been observed in our previous studies on the mono- and disilicon gold clusters.[14,15] However, our computational data (Fig. 2) suggest that isomers 1 and 2 are competitive with isomer 3 and could also contribute to the observed spectra. The valent electronic configurations of isomers 1 and 2 are $11a^2 12a^2 10b^2 13a^2$ [Fig. 5(a)] and $20a^2 21a^2 22a^2 23a^2$ [Fig. 5(b)], respectively. These two isomers are energetically almost degenerate, and indeed their calculated VDEs are consistent with the minor features x' and a', the more intense band b', providing evidence for the presence of these isomers experimentally. The stronger intensity of band b' could be due to either a stronger detachment cross section or contributions from $Si_{10}Au_2^-$ mass contamination.

VI. CHEMICAL BONDING IN $Si_3Au_3^{+/0/-}$ AND COMPARISON TO $Si_3H_3^{+/0/-}$

A. $Si_3Au_3^-$ and Si_3Au_3

The combined experimental and computational data clearly establish that isomers 1–3 of $Si_3Au_3^-$ are energetically competitive and coexist in the cluster beam. Structurally, all these three isomers have one common motif, i.e., the four-membered ring Si_3Au unit, with the other two Au atoms being arranged differently. The average Si–Si bond length varies from 2.27 Å in 3 to 2.40 Å in 1 and 2. However, the Si–Au distances in 1–3 appear similar, depending whether the Au is terminally bonded to Si or in bridging positions. Although isomer 3 is 0.29 eV higher in energy than isomer 1 at the current level of theory, we believe that the relative energies between isomers 1–3 are much closer. In isomer 3, the two terminal Au atoms on Si are bent towards the bridging Au atom with the $Au_{terminal}-Au_{bridge}$ distance of 3.43 Å, which is very much within the distance range of aurophilic interactions.[41] It is well known that DFT underestimates the strength of such interactions.[1] Therefore, we consider isomer 3 of $Si_3Au_3^-$ to be likely the global minimum on the basis of good agreement between the calculated VDEs of isomer 3 and the main PES features.

The valence MOs of isomers 1–3 are depicted in Fig. 5, whereas their corresponding Lewis chemical bonding pictures are shown in Fig. 6. The simple Lewis pictures are instructive despite the fact that they may not fully capture the nature of chemical bonding for such highly delocalized systems. As can be seen from Fig. 6, the core Si_3Au unit in isomers 1–3 each contains a Si–Au–Si 3c-2e bond, but the remaining two Au atoms arrange very differently. In isomer
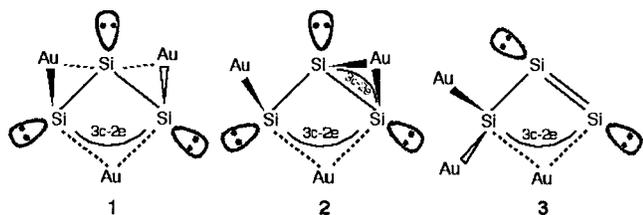
FIG. 6. Schematic valence bond description of the three lowest isomers (1–3) of $Si_3Au_3^-$.

1, the two out-of-plane Au atoms are *trans* to each other and are each primarily bonded to one Si atom with much weaker interactions to the third Si. In isomer 2, there is one $2c$-$2e$ terminal Si–Au bond and the other Au atom forms a second $3c$-$2e$ Si–Au–Si bond by bridging the remaining Si atoms. In isomer 3, there are two terminal Si–Au bonds and the bonding between the two remaining Si atoms may be viewed as a Si=Si double bond.

Similar chemical bonding features can be found in the corresponding hydrides (19–21), as depicted in Fig. 7, which are the three lowest energy isomers identified for $Si_3H_3^{0/-}$ from extensive computational search in Ref. 27. Although numerous other isomeric structures have been located on the potential energy surfaces of $Si_3H_3^{0/-}$, those are substantially higher in energy than 19–21.[27] One may roughly find the structural correspondence between $Si_3Au_3^-$ (Figs. 2 and 6) and $Si_3H_3^{0/-}$ (Fig. 7) as follows: $3 \leftrightarrow 19$, $2 \leftrightarrow 21$, and $1 \leftrightarrow 20$. Additional comparison between 1–3 and 19–21 and the subtle difference between the positions of Au and H in the respective structures will be discussed below in Sec. VI C. Interestingly, the global minimum 19 of $Si_3H_3^-$ corresponds to isomer 3, which is also the most likely global minimum for $Si_3Au_3^-$.

Chemical bonding in the Si_3Au_3 neutral isomers (7–9) is rather similar to that in the $Si_3Au_3^-$ anions (1–3), except that there is only one valence electron in the HOMO of the neutrals. And the three lowest energy structures of Si_3Au_3 are also similar to those of Si_3H_3.[27]

However, obvious structural differences exist between $Si_3Au_3^{+/0/-}$ and $Si_3H_3^{+/0/-}$, primarily due to the tendency of Au for bridge bonding. For example, in isomer 19 for the hydride, hydrogen does not bridge to form a $3c$-$2e$ Si–H–Si bond, instead it develops strong interaction with one Si by bonding terminally. In contrast, in isomer 3 of $Si_3Au_3^-$, one Au atom readily bridges two Si atoms and forms a Si_3Au ring structural unit via a $3c$-$2e$ Si–Au–Si bond. This phenomenon turns out to be rather general for all $Si_3Au_3^{+/0/-}$ species, because the core Si_3Au ring unit is commonly observed in the low-lying structures for $Si_3Au_3^-$, Si_3Au_3, and
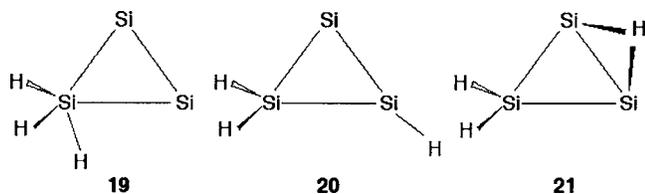

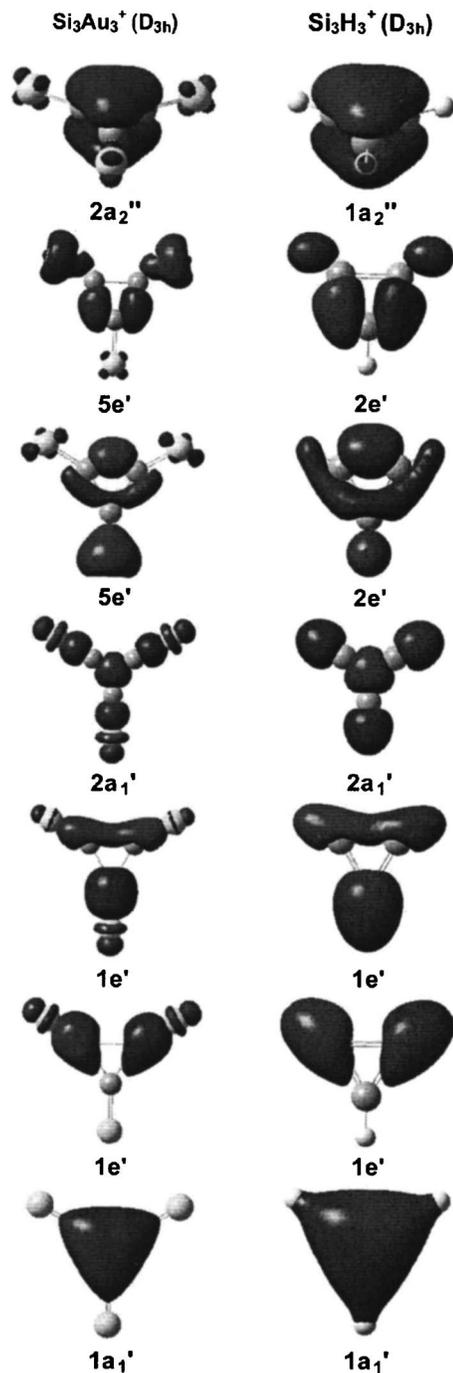FIG. 7. Schematic presentation of the three lowest energy isomers (19–21) of $Si_3H_3^{0/-}$.

FIG. 8. Comparison of the valence molecular orbitals of the most stable structures of $Si_3Au_3^+$ and $Si_3H_3^+$ in D_{3h} symmetry.

$Si_3Au_3^+$ (Figs. 2–4). Our previous work on the disilicon gold binary systems reveals similar structural behaviors of gold, which prefers to form bridges due to its larger size relative to hydrogen.[15] This observation indicates that for larger and more complicated Si–Au clusters, the detailed structures may deviate from the corresponding hydrides as a result of Au–Au interactions and the tendency of Au to form bridge bonds.

B. $Si_3Au_3^+$: A 2π aromatic silicon auride

$Si_3H_3^+$, the 2π aromatic cyclotrisilenylium ion, has been extensively studied among the three $Si_3H_3^{+/0/-}$ species.[21–26]

Recently, an aromatic cyclotrisilenylium ion with bulky substituents, which bears similarities with $Si_3H_3^+$, has been successfully synthesized.[26] Our extensive DFT structural search indeed located isomer 13 (D_{3h}, $^1A_1$) as the lowest energy isomer for $Si_3Au_3^+$ (Fig. 4), although lower symmetry isomer 14 (C_s, $^1A'$) is virtually degenerate in energy at the current level of theory. The Si–Si bond length (2.23 Å) in 13 is very close to those in the synthesized cyclotrisilenylium ion (2.211–2.221 Å) (Ref. 26) and lies in between the typical Si–Si single bond (2.3694–2.3762 Å) and the Si=Si double bond (2.1612 Å),[26] thus clearly indicating a delocalized electronic system. A comparison of the valence MOs between the aromatic cyclotrisilenylium ion $Si_3H_3^+$ and the aromatic cyclotrisilenylium auride ion $Si_3Au_3^+$ is shown in Fig. 8. As anticipated, there is a one-to-one correspondence in bonding between $Si_3Au_3^+$ and $Si_3H_3^+$. The HOMO in both species is the π bond, which is responsible for their aromaticity. The remaining MOs are simple and are responsible for the Si–Au(H) bonding and Si–Si σ bonding. Thus isomer 13 of $Si_3Au_3^+$ is a 2π aromatic molecule, analogous to the well established 2π aromatic cyclotrisilenylium ion $Si_3H_3^+$ and extending the Au/H analogy to an aromatic Si–Au cluster.

VII. CONCLUSIONS

A combined photoelectron spectroscopy and density functional study is carried out on the $Si_3Au_3^{+/0/-}$ clusters. Numerous PES spectral features are observed for $Si_3Au_3^-$. Extensive electronic structure calculations at the B3LYP level are carried out for $Si_3Au_3^-$, Si_3Au_3, and $Si_3Au_3^+$ to identify their low-lying structures. Several isomers of $Si_3Au_3^{+/0/-}$ are located, and the potential energy surfaces for $Si_3Au_3^{+/0/-}$ and $Si_3H_3^{+/0/-}$ appear to be similar. Comparison of the PES spectra and the computational data clearly establishes the coexistence of three structural isomers in the $Si_3Au_3^-$ cluster beam. For $Si_3Au_3^+$, the lowest energy isomer is found to be a highly symmetric D_{3h} species, which is aromatic with two delocalized π electrons, analogous to the well established cyclotrisilenylium ion, $Si_3H_3^+$. The larger size of the Au atoms tends to stabilize the bridging isomers as compared to the hydrides. The current study confirms and further extends the isolobal Au/H analogy in Si–Au binary clusters.

ACKNOWLEDGMENTS

[1] P. Pyykko, Angew. Chem., Int. Ed. **43**, 4412 (2004).
[2] P. Pyykko, Inorg. Chim. Acta **358**, 4113 (2005).
[3] H. Schmidbaur, S. Cronje, B. Djordjevic, and O. Schuster, Chem. Phys. **311**, 151 (2005).
[4] For a recent review, see P. Pyykko, Angew. Chem., Int. Ed. **41**, 3573 (2002).
[5] L. Gagliardi, J. Am. Chem. Soc. **125**, 7504 (2003).
[6] D. M. P. Mingos, Pure Appl. Chem. **52**, 705 (1980).
[7] K. P. Hall and D. M. P. Mingos, Prog. Inorg. Chem. **32**, 237 (1984).
[8] J. W. Lauher and K. Wald, J. Am. Chem. Soc. **103**, 7648 (1981).
[9] F. Scherbaum, A. Grohmann, G. Muller, and H. Schmidbaur, Angew. Chem., Int. Ed. **28**, 463 (1989).
[10] A. Grohmann, J. Riede, and H. Schmidbaur, Nature (London) **345**, 140 (1990).
[11] J. K. Burdett, O. Eisenstein, and W. B. Schweizer, Inorg. Chem. **33**, 3261 (1994).
[12] H. Schmidbaur, F. P. Gabbai, A. Schier, and J. Riede, Organometallics **14**, 4969 (1995).
[13] S. Kruger, M. Stener, M. Mayer, F. Nortemann, and N. Rosch, J. Mol. Struct.: THEOCHEM **527**, 63 (2000).
[14] B. Kiran, X. Li, H. J. Zhai, L. F. Cui, and L. S. Wang, Angew. Chem., Int. Ed. **43**, 2125 (2004).
[15] X. Li, B. Kiran, and L. S. Wang, J. Phys. Chem. A **109**, 4366 (2005).
[16] H. J. Zhai, L. S. Wang, D. Yu. Zubarev, and A. I. Boldyrev, J. Phys. Chem. A **110**, 1689 (2006).
[17] L. Gagliardi and P. Pyykko, Phys. Chem. Chem. Phys. **6**, 2904 (2004).
[18] T. K. Ghanty, J. Chem. Phys. **123**, 241101 (2005).
[19] J. M. Jasinski and S. M. Gates, Acc. Chem. Res. **24**, 9 (1991).
[20] C. J. Giunta, R. J. McCurdy, J. D. Chapple-Soko, and R. G. Gordon, J. Appl. Phys. **67**, 1062 (1990).
[21] A. Korkin, M. Gluhovstev, and P. v. R. Schleyer, Int. J. Quantum Chem. **46**, 137 (1993).
[22] E. D. Jemmis, G. N. Srinivas, J. Leszczynski, J. Kapp, A. A. Korkin, and P. v. R. Schleyer, J. Am. Chem. Soc. **117**, 11361 (1995).
[23] G. N. Srinivas, E. D. Jemmis, A. A. Korkin, and P. v. R. Schleyer, J. Phys. Chem. A **103**, 11034 (1999).
[24] S. P. So, Chem. Phys. Lett. **313**, 587 (1999).
[25] S. D. Li, H. L. Yu, H. S. Wu, and Z. H. Jin, J. Chem. Phys. **117**, 9543 (2002).
[26] M. Ichinohe, M. Igarashi, K. Sanuki, and A. Sekiguchi, J. Am. Chem. Soc. **127**, 9978 (2005).
[27] T. Saitoh, T. Naoe, and S. Ikuta, J. Chem. Phys. **122**, 204314 (2005).
[28] L. S. Wang, H. S. Cheng, and J. Fan, J. Chem. Phys. **102**, 9480 (1995).
[29] L. S. Wang and H. Wu, in *Cluster Materials*, Advances in Metal and Semiconductor Clusters Vol. 4, edited by M. A. Duncan (JAI, Greenwich, CT, 1998), p. 299.
[30] M. Dolg, U. Wedig, H. Stoll, and H. Preuss, J. Chem. Phys. **86**, 866 (1987).
[31] M. Dolg, in *Modern Methods and Algorithms of Quantum Chemistry*, NIC Series Vol. 1, edited by J. Grotendorst (Julich Research Center, Julich, Germany, 2000).
[32] T. Leininger, A. Berning, A. Nicklass, H. Stoll, H. J. Werner, and H. J. Flad, Chem. Phys. **217**, 19 (1997).
[33] W. Kuchle, M. Dolg, H. Stoll, and H. Preuss, *Pseudopotentials of the Stuttgart/Dresden Group 1998* revision 11 August 1998; see worldwide website: http://www.theochem.uni-stuttgart.de/pseudopotentiale
[34] J. M. L. Martin and A. Sundermann, J. Chem. Phys. **114**, 3408 (2001).
[35] R. A. Kendall, T. H. Dunning, Jr., and R. J. Harrison, J. Chem. Phys. **96**, 6796 (1992).
[36] A. D. Becke, J. Chem. Phys. **98**, 5648 (1993).
[37] C. T. Lee, W. T. Yang, and R. G. Parr, Phys. Rev. B **37**, 785 (1988).
[38] P. J. Stephens, F. J. Devlin, C. F. Chabalowski, and M. J. Frisch, J. Phys. Chem. **98**, 11623 (1994).
[39] M. E. Casida, C. Jamorski, K. C. Casida, and D. R. Salahub, J. Chem. Phys. **108**, 4439 (1998).
[40] M. J. Frisch, G. W. Trucks, H. B. Schlegel *et al.*, GAUSSIAN 03, Revision B.04, Gaussian, Inc., Pittsburgh, PA, 2003.
[41] H. Schmidbaur, Gold Bull. **33**, 3 (2000).